LEVEL II

AD

AD A102389

RESPONSE OF A
TWO-FOR-ONE TACTICAL SHELTER
TO RACKING LOADS

BY ARTHUR R. JOHNSON

DTIC
ELECTE

AUG 4 1981

A

JANUARY 1981

UNITED STATES ARMY
NATICK RESEARCH and DEVELOPMENT LABORATORIES
NATICK, MASSACHUSETTS 01760

AERO-MECHANICAL ENGINEERING LABORATORY

81 8 04 009

DTIC FILE COPY

Approved for public release; distribution unlimited.

Citation of trade names in this report does not
constitute an official indorsement or approval of the
use of such items.

Destroy this report when no longer needed. Do not
return it to the originator.

SECURITY CLASSIFICATION OF THIS PAGE (When Data Entered)

REPORT DOCUMENTATION PAGE		READ INSTRUCTIONS BEFORE COMPLETING FORM
1. REPORT NUMBER	2. GOVT ACCESSION NO. AD-A102389	3. RECIPIENT'S CATALOG NUMBER
4. TITLE (and Subtitle) RESPONSE OF A TWO-FOR-ONE TACTICAL SHELTER TO RACKING LOADS.		5. TYPE OF REPORT & PERIOD COVERED August 1980 to January 1981
		6. PERFORMING ORG. REPORT NUMBER
7. AUTHOR(s) Arthur R. Johnson		8. CONTRACT OR GRANT NUMBER(s)
9. PERFORMING ORGANIZATION NAME AND ADDRESS US Army Natick Research & Development Laboratories ATTN: DRDNA—UE Natick, MA 01760		10. PROGRAM ELEMENT, PROJECT, TASK AREA & WORK UNIT NUMBERS 62723A 1L162723A427 01003BG
11. CONTROLLING OFFICE NAME AND ADDRESS US Army Natick Research & Development Laboratories ATTN: DRDNA—UE Natick, MA 01760		12. REPORT DATE January 1981
		13. NUMBER OF PAGES 41
14. MONITORING AGENCY NAME & ADDRESS(if different from Controlling Office)		15. SECURITY CLASS. (of this report) UNCLASSIFIED
		15a. DECLASSIFICATION/DOWNGRADING SCHEDULE

16. DISTRIBUTION STATEMENT (of this Report)

Approved for public release; distribution unlimited.

17. DISTRIBUTION STATEMENT (of the abstract entered in Block 20, if different from Report)

18. SUPPLEMENTARY NOTES

19. KEY WORDS (Continue on reverse side if necessary and identify by block number)

ISO SHELTERS	FINITE ELEMENTS	MODELS
ARMY SHELTERS	CONTAINERS	BEAM (STRUCTURAL)
STRUCTURAL BEHAVIOR	TACTICAL SHELTERS	LOADS (FORCES)
STRESSES	LOAD CARRYING	

20. ABSTRACT (Continue on reverse side if necessary and identify by block number)

A finite element model of a two-for-one tactical shelter is presented. The model is compatible with the COSMIC*NASTRAN finite element program. Both beam and composite plate elements are used in the model. The geometric properties of the beams are given in tables. The shelter's response to racking loads is calculated for one transverse loading condition on each end of the shelter. Two computer models are used to analyze the response at the personnel door end and seven models for the cargo door end. The models represent different methods for using the doors as load-carrying members. Stresses in the doorframes, loads on

DD FORM 1473 EDITION OF 1 NOV 65 IS OBSOLETE

20. Abstract (cont'd)

the door hinges, and loads on the corners of the doors are all determined and discussed. The computer models and the relation between the computed responses and the actual structural response are also discussed. It is shown that the framework cannot sustain the racking load without using the doors as load-carrying members, and when the doors are used, the door hinge loads are large.

PREFACE

The US Army Natick Research and Development Laboratories are developing a family of rigid wall tactical shelters. This study is one of a series of in-house analytical and numerical studies being made to develop a detailed engineering understanding of how tactical shelters respond to environmental loadings. Two other reports in this series can be obtained from NTIS. Their title and order numbers are "Finite Element Analysis of a Statically Loaded ISO Tactical Shelter," AD-A075807, and "A Study of Transversely Loaded Panels Used in Tactical Shelters," AD-A085138. The work reported in this study is of a applied engineering character and was initiated after two contractor-supplied two-for-one shelters failed to pass the transverse racking tests. The results of this effort explain why the shelter failed the test and suggest modifications to improve the shelter's ability to resist the transverse racking loads.

The rigid wall tactical shelter fabrication drawings use U.S. Customary units for dimensioning. This report utilized these drawings and is also, therefore, in British units. A conversion table between U.S. Customary and SI units is included on page 7.

The author would like to thank Mr. John Roche and Mr. James McLaughlin for their assistance in processing computer runs and obtaining data for this study.

Accession for
NTIS GRA&I
DTIC TAB
Unannounced
Justification

Distribution/
Availability
A.

1

TABLE OF CONTENTS

3

LIST OF ILLUSTRATIONS

4

LIST OF ILLUSTRATIONS (cont'd)

LIST OF ILLUSTRATIONS (cont'd)

Table 1. Conversion table. U.S. Customary units to SI units

Quantity	U.S. Customary	SI Units	To convert U.S. Customary units to SI units multiply by
Mass	pounds mass	kilograms	0.455
Force	pounds force	newtons	4.45
Length	inch	meter	0.0254
	foot	meter	0.305
	yard	meter	0.91
Area	square inch	square meters	6.45×10^{-4}
	square foot	square meters	0.093
Volume	cubic inches	cubic meters	1.64×10^{-5}
	cubic feet	cubic meters	0.0283
Density	pounds per cubic inch	kilograms per cubic meter	2.77×10^{4}
	ounces	grams per square meter	34
Tension	pounds per inch	newtons per meter	176
Moment of Inertia	(inches)^4	(meters)^4	4.1×10^{-7}
Modulus of Elasticity and Stress	pounds per square inch	newtons per square meter	6.89×10^{3}

7

RESPONSE OF A TWO–FOR–ONE TACTICAL
SHELTER TO RACKING LOADS

1. INTRODUCTION

Extensive testing of prototype two-for-one tactical shelters indicated that the shelters were not able to pass the ISO racking tests without sustaining physical damage. It then became of interest to understand how the two-for-one tactical shelters respond to ISO racking loads. The calculations made in this study were directed at evaluating the load-carrying capability of the current design. The analytical study is broad enough so that the mechanism of load distribution in the frame-and-panel end wall can be understood for a number of modifications of the end walls. Nine different conditions were considered. Two conditions for the personnel door end and seven conditions for the cargo door end.

In Section 2 of this study the finite element model of the two-for-one tactical shelter is described. The nodal points, beams elements, and plate elements are identified. Their orientation in space is shown and their geometric properties are given. In Section 3 the details of each model of the end walls are discussed. Also, scaled plots of the deformed end walls, and brief descriptions of the stresses in the end wall frames are given for each case analyzed. In Section 4 of this study a summary of the door hinge loads is given. The last section of this study contains comments on the limitations of the analysis and on the design of the end walls.

2. THE GLOBAL FINITE ELEMENT MODEL

The finite element model used is a modification of an undocumented finite element model received with the first prototype Army Standard Family One-Side Expandable Shelter. The model was compatible with MSC*NASTRAN only and it contained errors. Most of the errors involved incorrect orientation of beam elements. The panel close-out extrusions which were not in the model were included in the new model and the model was made compatible with level 17.5 COSMIC*NASTRAN.[1,2] Figure 1 shows the components of the shelter included in the finite element model (the door frames are built into the end wall panels). The mesh used to discretize the shelter is shown in Figure 2 along with the nodal (GRID) point identification numbers. The sandwich panels were modeled with CQUAD1 rectangular plate elements. These plate elements model bending, transverse shear, and inplane membrane responses of the sandwich panel. The plate elements are shown in Figure 3 and the beam elements used to model the framework are shown in Figure 4. These frame members include the floor frame, the roof hat beam, the corner posts and the cargo doorframe. The beam elements used to model the panel close-out extrusions are shown in Figure 5. The personnel doorframe is included in the close-out extrusion beam elements.

[1] H. G. Schaeffer. MSC/NASTRAN Static and Normal Modes Analysis. Wallace Press, Inc., Milford, New Hampshire, 1979.

[2] The NASTRAN Theoretical Manual (Level 17.5). COSMIC, University of Georgia, Athens, Georgia, December 1978.

9

For the GRID points associated only with plate elements the rotational degrees of freedom about the normal to the plate elements were eliminated on the GRID cards (which define active degrees of freedom) when no beam elements were connected to the GRID points. The components of the shelter were connected by writing the appropriate equations of constraint and using the MPC cards in NASTRAN to enforce them. Except for the doors, the constraint equations represent a rigid attachment of the degrees of freedom at the boundaries between the components of the shelter. The connection of the doors to the doorframes is discussed in Section 3 of this study.

The geometric properties of the beams are given in Tables 1 to 4. There were 17 different cross sections among the frame members used in the finite element model. The shapes of the cross sections, the local element coordinates at end A of the element, and the stress recovery points used for obtaining the bending stresses are also given in Tables 2 to 5.

The finite element model used in this study is useful for computing the overall structural behavior of the shelter. However, several comments about the model should be made. The nodes used to represent the discretization of the personnel door end wall did not line up with the nodes used to discretize the roof and the floor. This had no effect on the model of the frame since NASTRAN has provisions for treating such cases when beam elements are used. No special treatment was given to the plate elements here. Thus, the plate elements near the top and bottom center of the personnel door end wall are not of the correct size. The author has chosen to leave the model this way since correction of the problem would result in elements that are nearly congruent to the current elements. The resulting element stiffness matrices would then also be nearly equal. Next, the model of the roof, floor, side walls, and personnel door wall included the effects of the panel close-out extrusions. However, the close-out extrusions were not included in the models of the doors. Thus, in the actual structure the doors will be slightly stiffer than indicated in this study. The last comment on the model relates to numerical accuracy. The effect of the discretization on the numerical results was not determined. However, the results from other studies conducted by the author[3,4] indicate that this model is sufficiently accurate for predicting the overall structural behavior of the shelter.

[3]Arthur R. Johnson. A Study of Transversely Loaded Panels Used in Tactical Shelters. Technical Report NATICK/TR—80/006, US Army Natick Research & Development Command, Natick, MA, 1979 (AD—A085138).

[4]A. R. Johnson and V. P. Ciras. Finite Element Analysis of a Statically Loaded ISO Tactical Shelter. Technical Report Natick/TR—79/023, US Army Natick Research & Development Command, Natick, MA, (AD—A075807).

3. MODELING AND ANALYSES OF END WALLS SUBJECTED TO RACKING LOADS

The doors used in the end walls do not fit tightly into the doorframes. There are nonmetallic shims attached to the corners of the doors and gaps ranging in size from 1 8 inch to 1/4 inch exist between the shims and the doorframe. Thus, when the shelter is deformed the doors move until they come in contact with the doorframe. During testing it was determined that the doors contact the doorframe at low loads. Displacement data taken from the finite element analyses made in this study predict that if the gaps are about 1/8 inch then a racking load of 8.9×10^3 lb will close the gaps at the personnel door end and a load of 5.9×10^3 lb will close the gaps at the cargo door end. A nonlinear analysis which would correctly model all the gaps was considered beyond the scope of this study. Instead, two sets of internal structural forces and stresses were sought by modeling the end wall doorframe interaction two ways. First, the doors were assumed not to contact the doorframe at the door corners (doors were attached to the doorframe only at the hinge locations). Second, the doors were assumed to be shimmed tightly so that no gaps existed. The structural analysis data from both of these situations was evaluated assuming that the actual structural response would yield results between the results for these two models. At the cargo door end further models were constructed to investigate the advantages associated with several methods of connecting the doors to each other and to the doorframe.

a. Modeling and Analysis of Personnel Door End Wall

The racking load used to analyze the personnel door end wall's response to the racking test was a 33.6×10^3 lb static load applied at node 100 in the negative y direction. The shelter was pinned at all four bottom ISO fittings. That is, the x, y, and z translations at nodes 400, 410, 444, and 454 were enforced to zero. Two models, described below, of the personnel door end wall were made, and the deformations, stresses, and element nodal forces were determined for each model. The connections between the personnel door and the doorframe for the first case analyzed are shown in Figure 6. The connections represent the door being attached at the hinges and being restricted from swinging open. There is no contact between the door and the doorframe at the door's corners. This model represents the case when the gaps between the door and the doorframe are so large that when the shelter deforms, the gap is not closed by the relative movement between the door and the doorframe. The deformed body plot is shown in Figure 7. The apparent overlapping of the door and the end wall exists because the door and doorframe nodes are at the same initial location in the finite element model. The plot indicates that the door header beam will be curved up on the left and down on the right when the door does not interact with the header beam.

The connections between the door and the doorframe for the second case analyzed are shown in Figure 8; these connections cause the door to deform with the doorframe and thus stiffen the end wall. When these connections are used the numerical results indicate that compressive interactions exist between the door and the doorframe at the top left and bottom right corners of the door, and tensile interactions at the top right and bottom left corners of the door. To simulate this case in the actual structure it would be necessary to restrain the door and the doorframe from moving apart in the corners when tensile interactions were observed. The deformed body plot is shown in Figure 9. The plot indicates that the header beam is not deformed as in the previous case. Instead, in this case, the door restricts the header beam from bending to the extent it did in the previous case.

11

Some of the maximum stresses in the loaded doorframe for each case are listed in Table 6. The frame members were fabricated from 6061-T6 which has a yield strength of about 35×10^3 psi. Then, for the frame members considered in Table 6, case 1 is not acceptable. It is interesting to note that the highest stresses for case 1 are at the top left corner of the doorframe which is where the frame failed in an actual test, see Figure 10. The results for the actual structure would not be as severe as those indicated in case 1. When the shelter deforms the gaps between the door and the doorframe close. The door and the doorframe then interact in a manner similar to that predicted by case 2 and the stresses listed for case 2 are at an allowable level. This does not necessarily imply that designing for case 2 will yield an acceptable structure. Hinge forces, stress concentrations near joints, and joint loads must also be considered. The hinge forces are discussed in Section 4 of this study and an evaluation of the stress concentrations near the joints is beyond the scope of this effort.

b. Modeling and Analysis of the Cargo Door End Wall

The racking load used to analyze the cargo door end wall was a 33.6×10^3 lb static load applied at node 110 in the negative y direction. The shelter was pinned again at all four bottom ISO fittings. Six models of the end wall were made. The end wall models, the deformed body plots, and the maximum frame stresses are presented.

The constraints used to model cases 3 through 9 are shown in Figures 11, 13, 15, 17, 19, 21 and 23, respectively. In case 3 the doors were attached to the doorframe at the hinge points and were restricted from swinging open. The case 3 constraints represent the case when large gaps exist between the cargo doors and between the cargo doors and the doorframe. The deformations are shown in Figure 12. The deformation plot indicates that the doors will slide relative to each other. The external frame will be carrying the load (doors moved without deforming) and the header beam will contain a point of inflection at the center. In case 4 constraints were added to simulate the doors being attached to the doorframe and the floor in the corners of the hinged sides. The doors slide relative to each other. One door jams against the header beam and the other door jams against the floor. The deformed body plot for case 4 is given in Figure 14. For these constraints the header beam and the floor will tend to bow up and down, respectively. The case 5 constraints were made to simulate the case when the right door in Figure 15 is attached to the header beam at the top and to the floor at the bottom, and both doors are attached to the doorframe in the corners on the hinged sides. The deformations for case 5 are shown in Figure 16. When the right-hand door is attached at the top to the header beam and at the bottom to the floor both the header beam and the floor will tend to bow in the same direction. The case 6 constraints simulate the case when both doors were attached top and bottom to the header beam and the floor, respectively, and again the corners of the doors on the hinged side were attached to the doorframe. The deformed body plot is given in Figure 18 and indicates that the doors will be load-carrying members in this case (the doors are distorted). The constraints for case 7 simulate the case when the doors are tied at the top and bottom, but unlike cases 4, 5, and 6, the constraints simulating the doors being attached to the doorframe in the corners on the hinged sides were not included. The deformation plot for case 7 is given in Figure 20 and indicates that both the doors and the doorframe are carrying loads, since both are distorted. The constraints for case 8 simulate both doors being attached at the top and bottom center

12

to the header beam and floor, respectively. Also, there were no corner constraints on the hinged sides of the doors. Thus, except for the hinged corners, case 8 is similar to case 6. The deformed body plot for case 8 is shown in Figure 22. Again, both the doors and doorframe are distorted, indicating that they are both resisting the load. The constraints for the last model, case 9, are the same as those of case 6 except the corner constraints (which caused tensile loads to exist between the doorframe corners and the door corners in case 6) were not included, see Figure 23. Thus, case 9 represents the case when both doors are firmly attached, top and bottom, to the doorframe and the doors are tightly shimmed at the doorframe corners. The deformed body plot for case 9 is shown in Figure 24.

A summary of the maximum combined bending and axial stresses in the cargo doorframe is given in Table 7. The results indicate that when the doors are not distorted (cases 3, 4, and 5) the stresses in the doorframe are well above the yield value. Element numbers 604 through 607 (the header beam) are highly stressed. However, when the doors are distorted (cases 6, 7, 8, and 9) the combined stresses in the doorframe beams are at an allowable level. Then, Table 7 and Figures 11 to 24 demonstrate numerically the shelter's response when the cargo doors are utilized, in several ways, as load-carrying members. In cases 4, 5 and 6 tensile reactions were obtained at varying locations on the door corners. That is, the corner constraints on the hinged sides did not always represent the doors jamming into the doorframe corners, but sometimes represented the door pulling on the doorframe in a corner. In case 9 there were no tensile reactions at the doorframe corners. The results shown in Table 7 indicate that utilizing the cargo doors as load-carrying members by connecting them to the doorframe at the top and bottom center of the end wall can significantly reduce the stresses in the doorframe.

4. LOADS ON HINGES AND DOOR CORNERS

The finite element model used in this study has three hinge connections between each door and the doorframe. Three hinges were proposed for the original design, and the finite element discretization of the end walls was based on the original proposal of three hinges. The current structural design has four hinges between each door and the doorframe. The results discussed here apply to the three-hinge design.

The forces on the door corners and hinges are listed in Tables 8 and 9 for the personnel and cargo door ends, respectively. Figure 25 shows the locations of the nodes on the boundary of the doors and is intended to be used as a visual aid for the data in Tables 8 and 9. The data for the personnel door end indicates that there is a large difference in the hinge loads between cases 3 and 4. The largest change is at the top hinge (node 503). Also, the corner loads at node 500 are the largest reactions. In fact, the Z-component of the door corner reaction at node 500 is about 2/3 the value of the applied load. At the cargo door end the largest hinge loads occur in cases 7 and 8. In terms of the constraints on the cargo doors, the similarities between cases 7 and 8 are that the doors are attached to each other in shear, and that there are no corner reactions allowed between the doors and the doorframe. If the stresses are also considered, cases 6 and 9 are attractive. The hinge loads in case 6 are lower than those of case 9. In terms of a practical design, however, case 4 is difficult to implement. This is because the doorframe corners must be made to interact in both tension and compression

with the doors. Case 9 is closely related to the case when the doors are shimmed at the doorframe corners and attached to the doorframe at the top and bottom center of the end wall.

5. CONCLUSION

Nine structural models were developed to obtain structural analysis data on the response of a two-for-one tactical shelter subjected to racking loads. The results of the analyses indicate that the shelter will not pass the transverse racking test if the doors are not used as load-carrying members. Of the structural models utilizing the doors as load-carrying members those models which also have the doors shimmed yield the best results. Also, when the doors are used, the hinge loads will be large. The actual nonlinear response of the shelter (response with gaps) was not determined in this study. Instead, a number of linear responses were determined which provide a practical understanding of how the components of the shelter respond when the shelter is subjected to a transverse racking load. There is enough information in this report to justify that the end walls should be redesigned. That is, the failures of the shelters tested were due to the fact that the shelters were underdesigned for the loading requirements.

6. RECOMMENDATIONS

The end walls should be redesigned. In the new designs the doors should be used with the doorframes to help carry the transverse racking loads. The free vertical edges of the personnel door and both cargo doors should be attached to both the top and bottom of the doorframes. Shims should be used at the door corners and an effort should be made to keep the gaps between the door-mounted shims and the doorframe as small as possible (to simulate case 2 at the personnel door end and case 9 at the cargo door end). Further analyses should be made to determine the hinge and door corner reactions for the case when four hinges connect each door to the doorframe. The doors and hinges should then be designed to withstand the required reactions. Alternatively, using the numerical data on the hinge loads and door-to-doorframe interaction loads provided in this study as general guidance, new prototype end walls may be designed and tested.

14
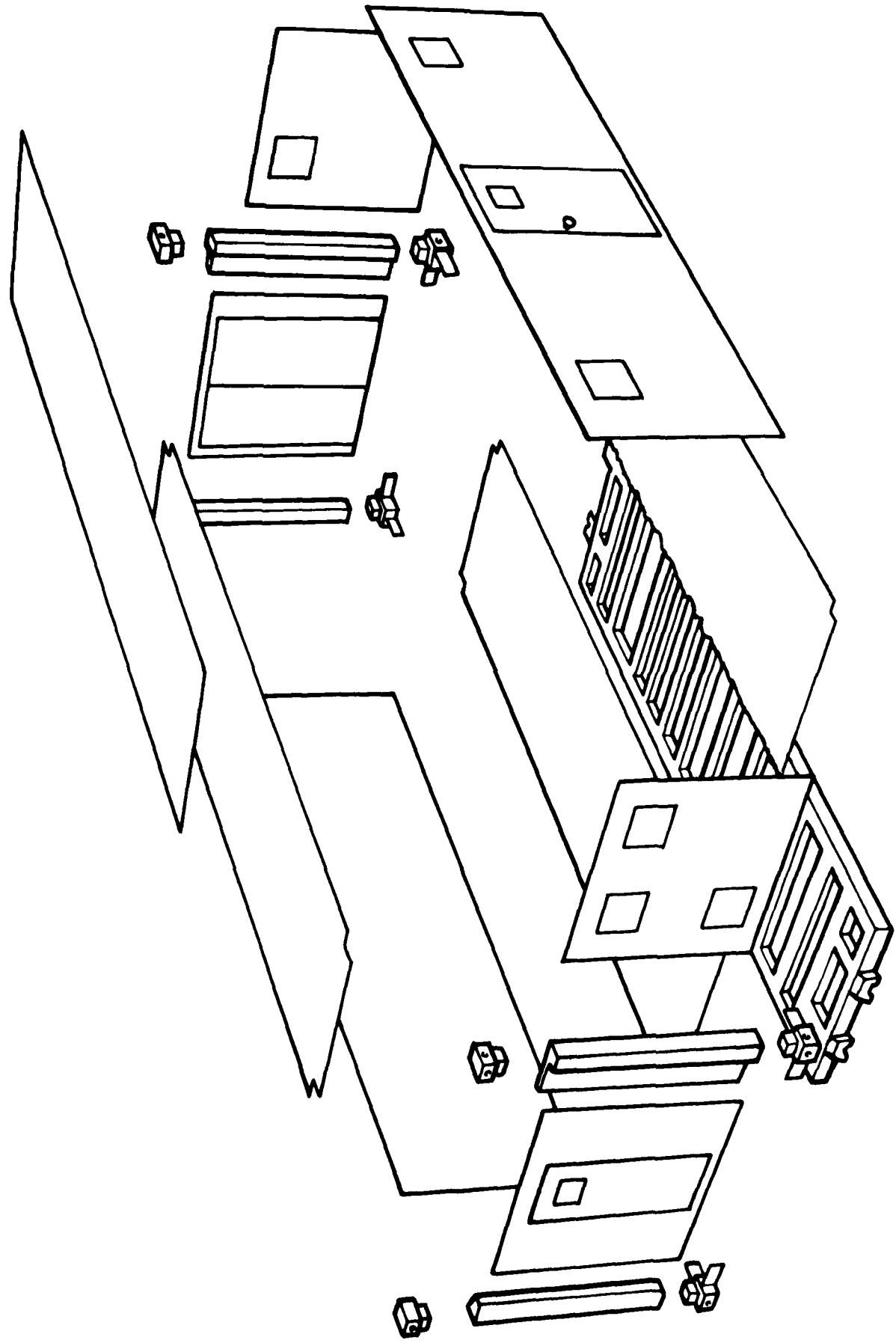
Figure 1. Shelter components used in finite element model.
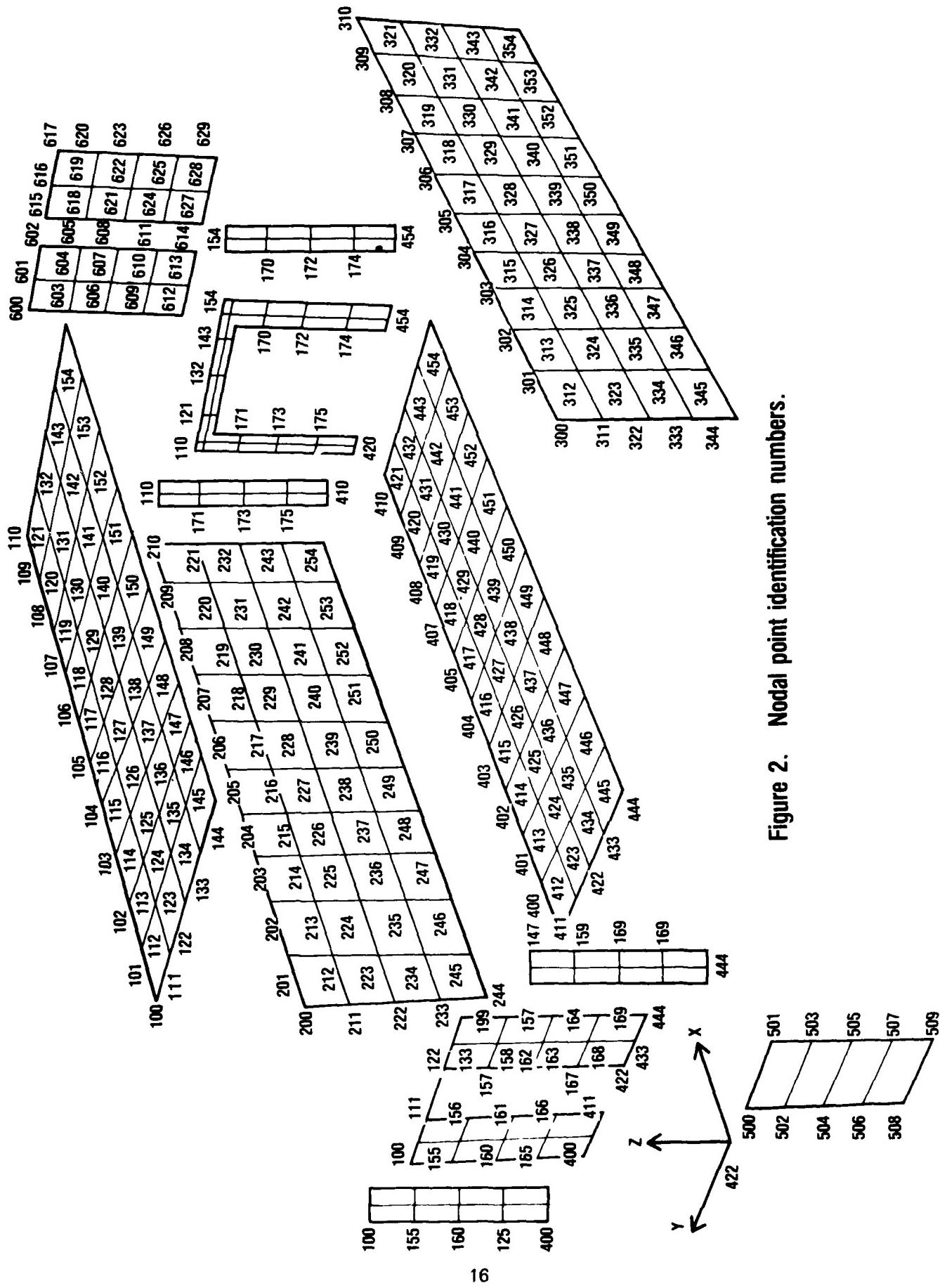
Figure 2. Nodal point identification numbers.

16
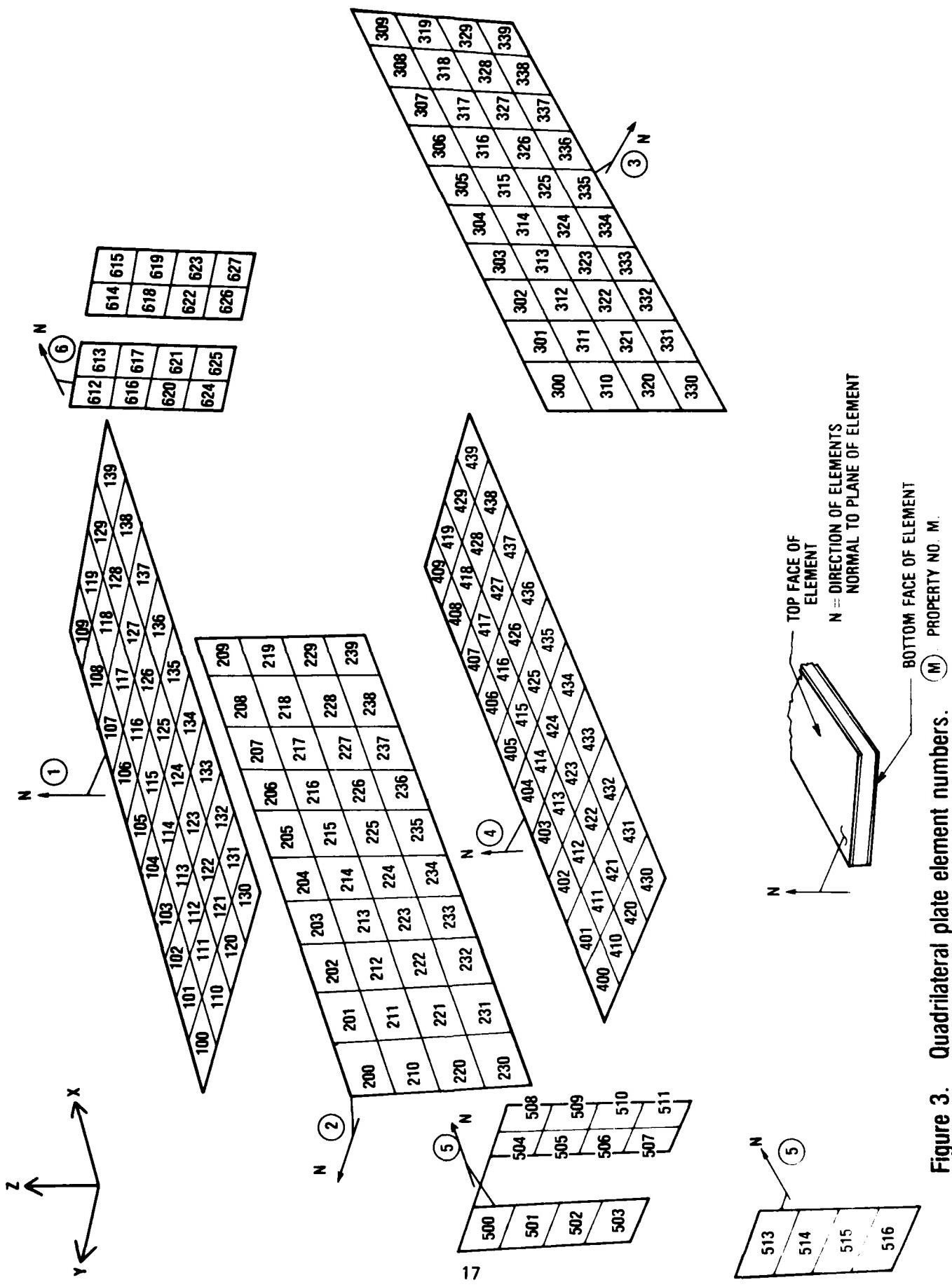
Figure 3. Quadrilateral plate element numbers.
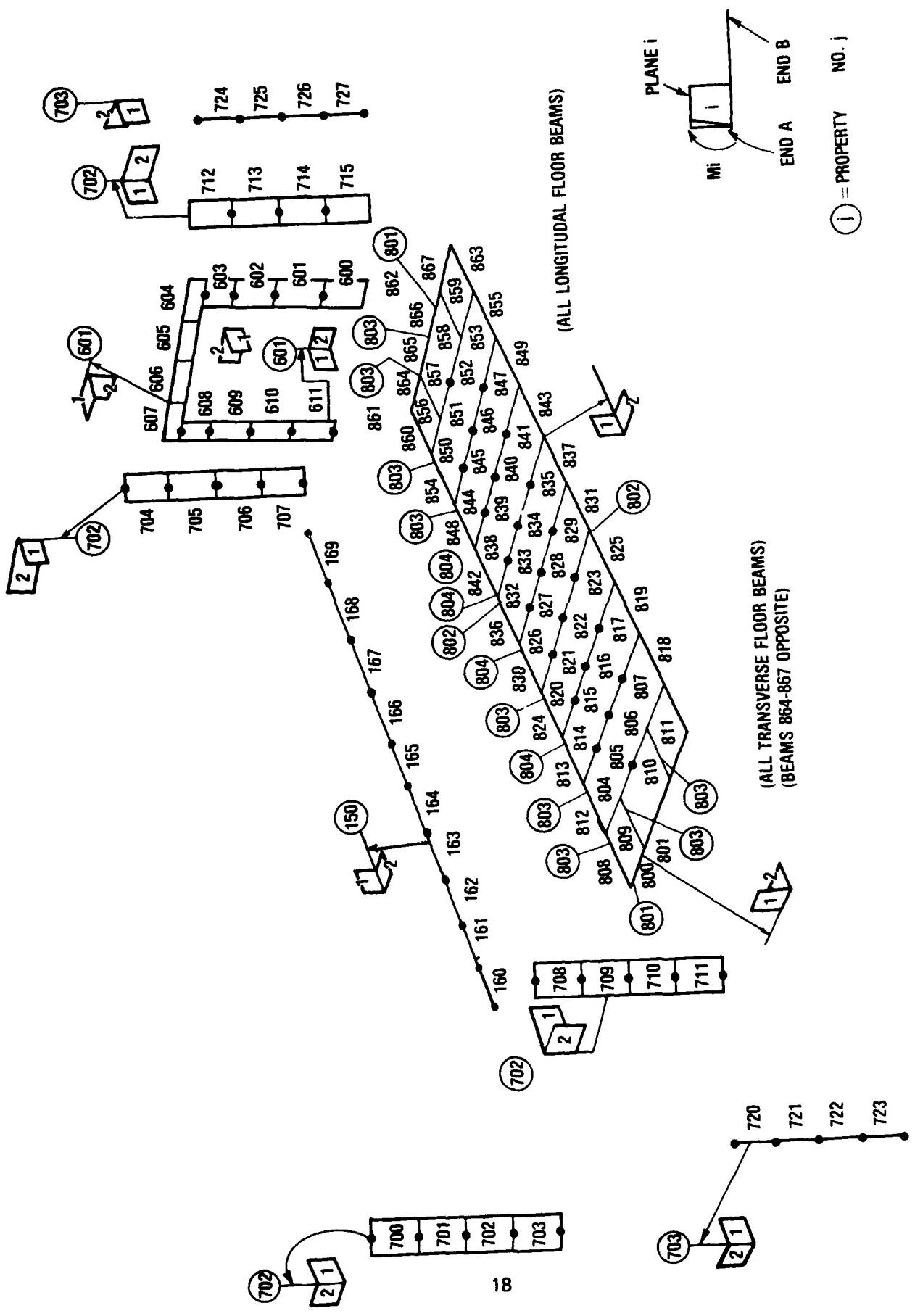
Figure 4. Beam element numbers for frame.

18
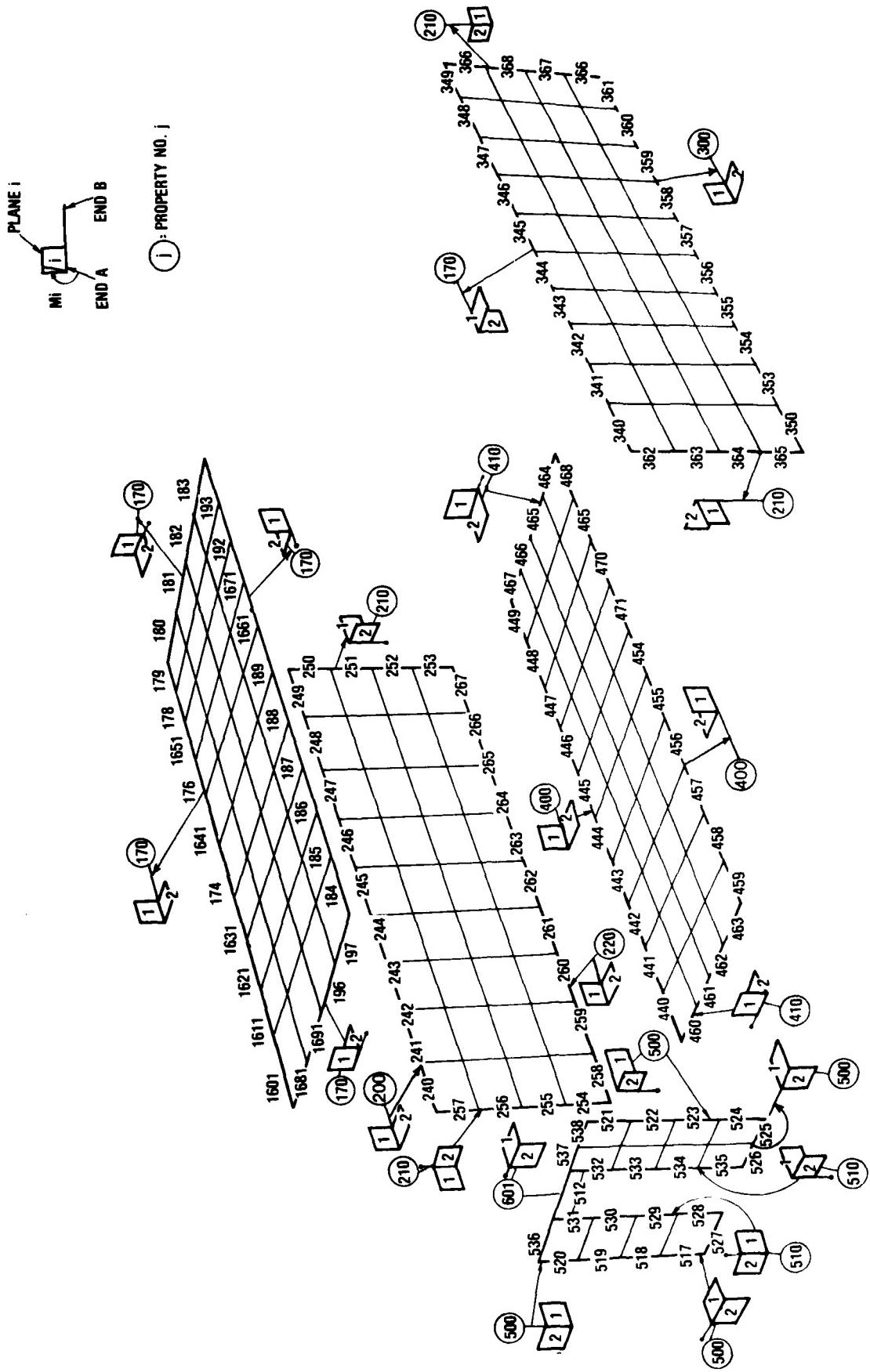
Figure 5. Beam element numbers for panel close-out extrusions.
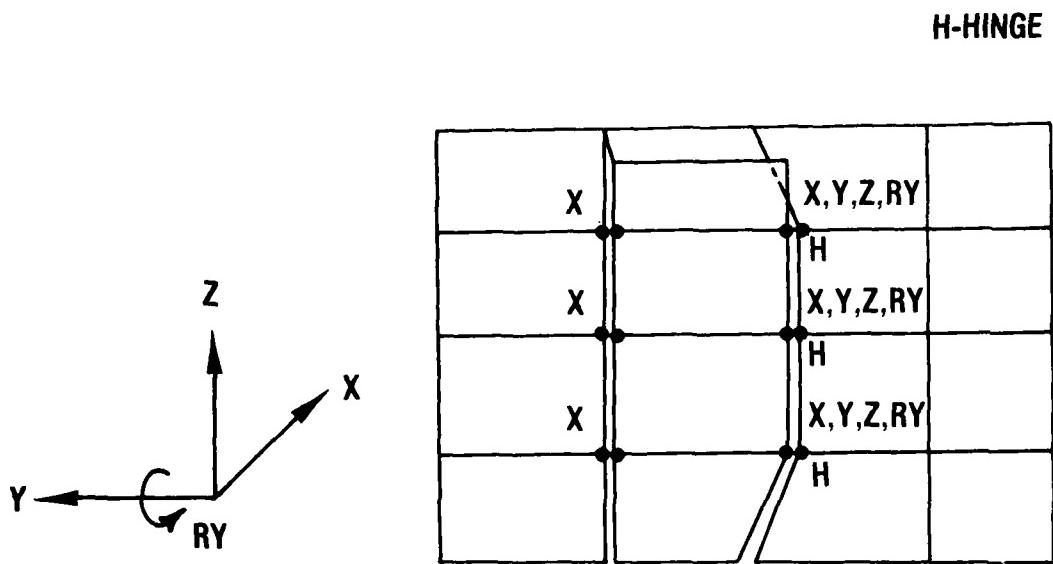
Figure 6. Case 1. Personnel door endwall, connected degrees of freedom between door and doorframe.
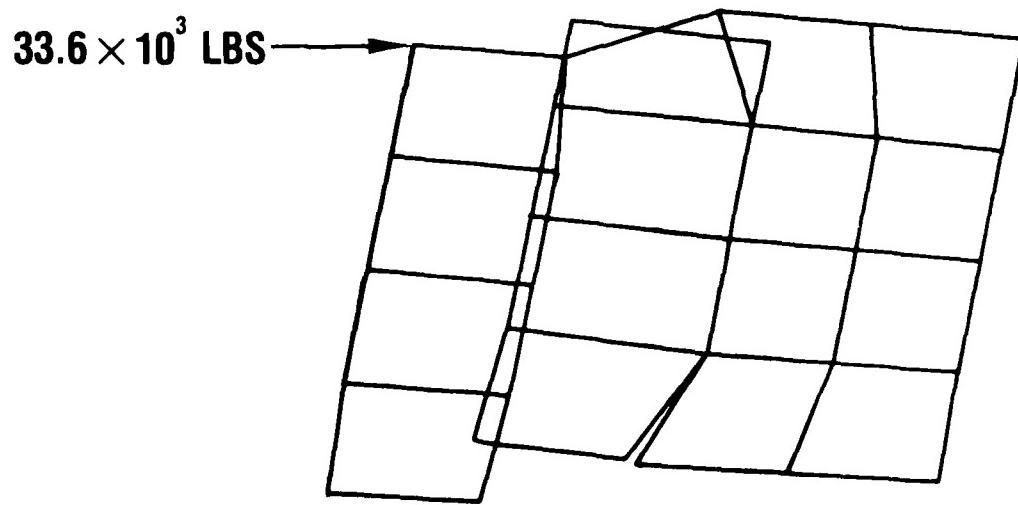
**Figure 7.** Case 1. Personnel door endwall, deformed body plot.
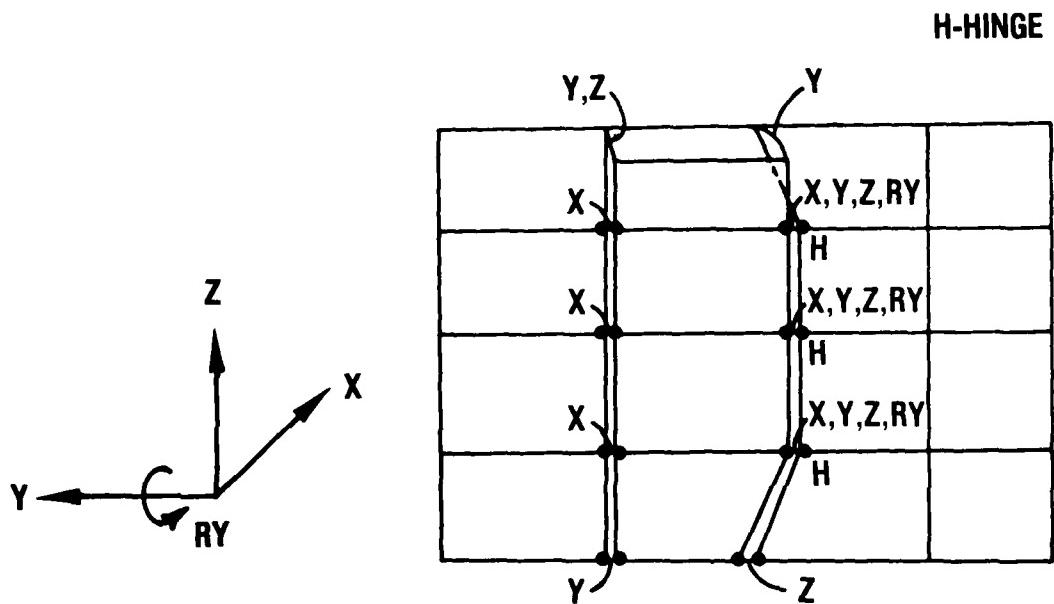
Figure 8.   Case 2. Personnel door endwall, connected degrees of freedom between door and doorframe.
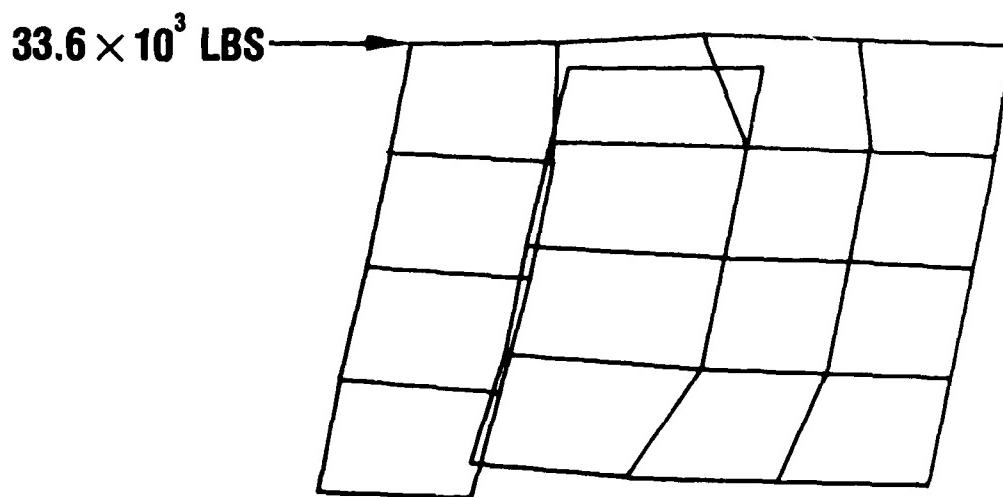
Figure 9.   Case 2. Personnel door endwall, deformed body plot.
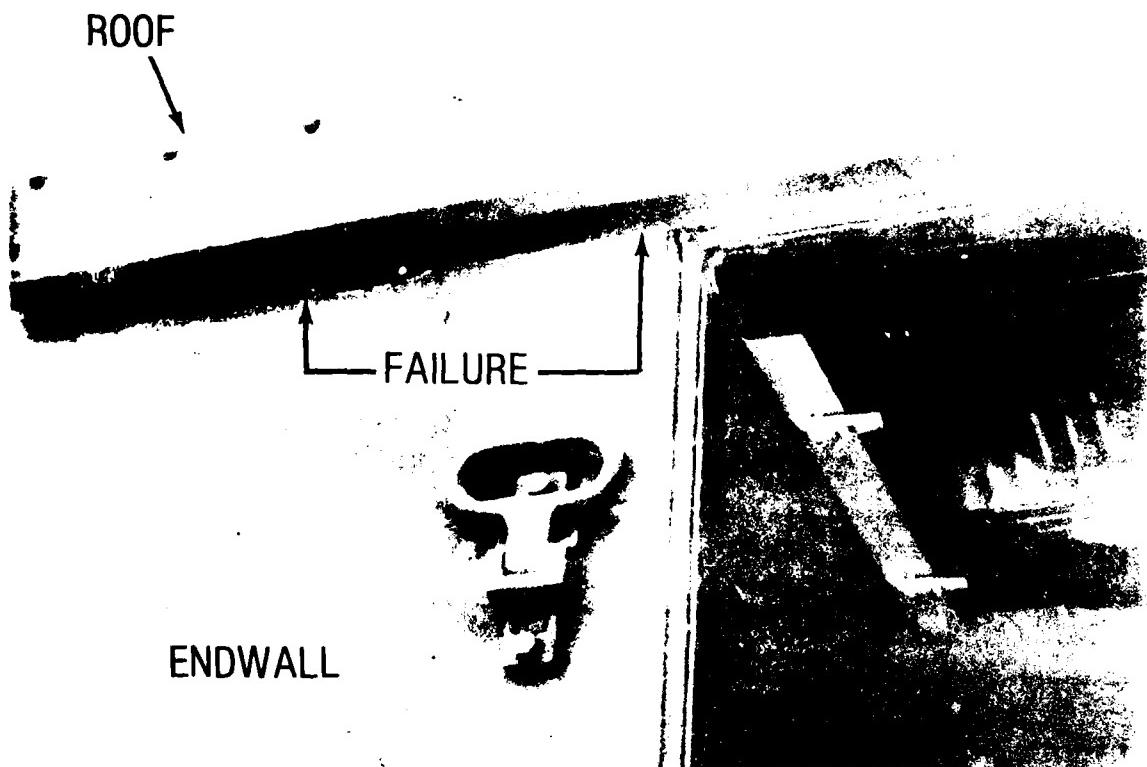
FIGURE 10. FAILURE OF TOP LEFT CORNER OF PERSONNEL DOORFRAME.
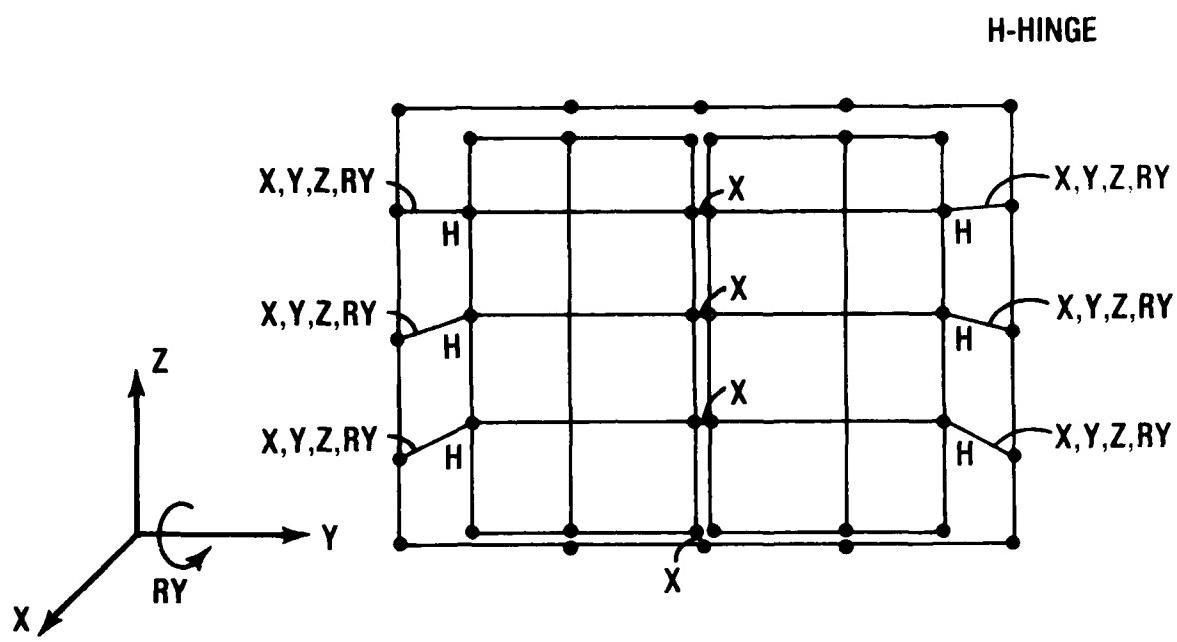
Figure 11. Case 3. Cargo door endwall, connected degrees of freedom between door and doorframe.
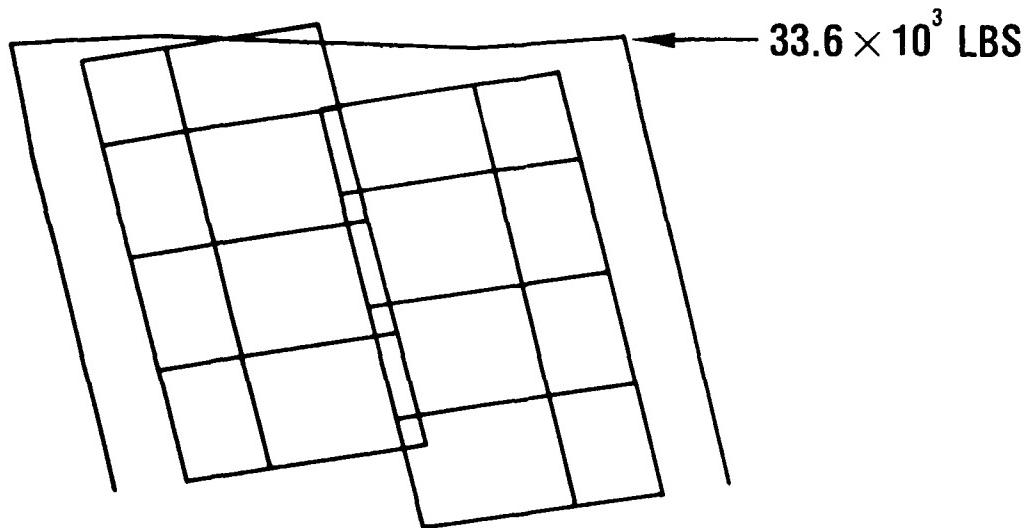
**Figure 12.** Case 3. Cargo door endwall, deformed body plot.
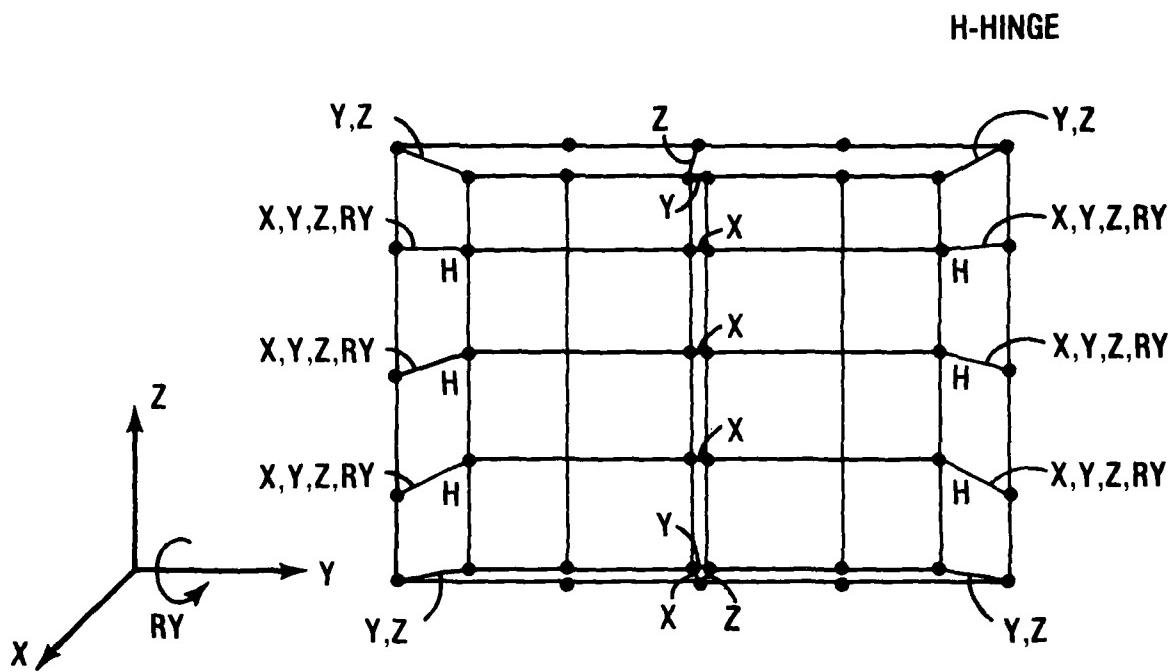
Figure 13. Case 4. Cargo door endwall, connected degrees of freedom between door and doorframe.
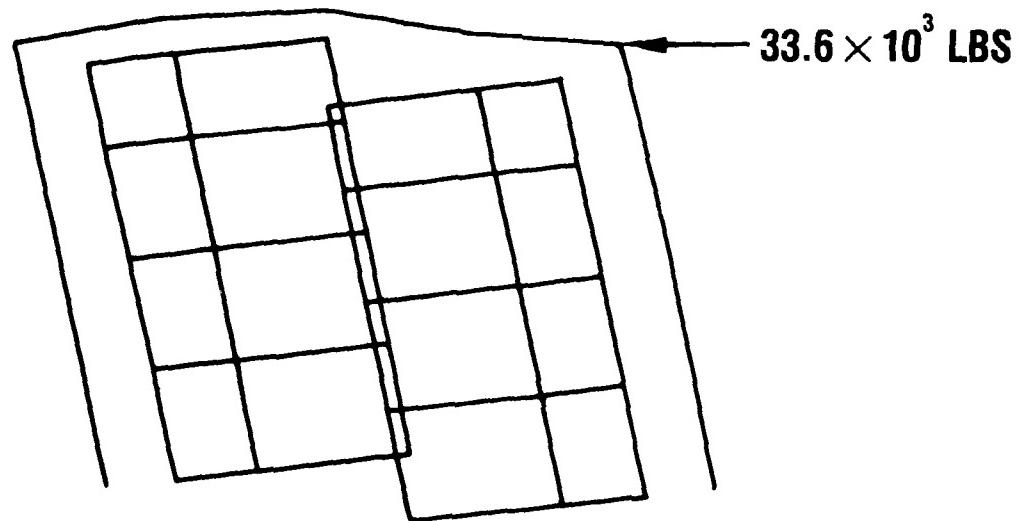
Figure 14. Case 4. Cargo door endwall, deformed body plot.
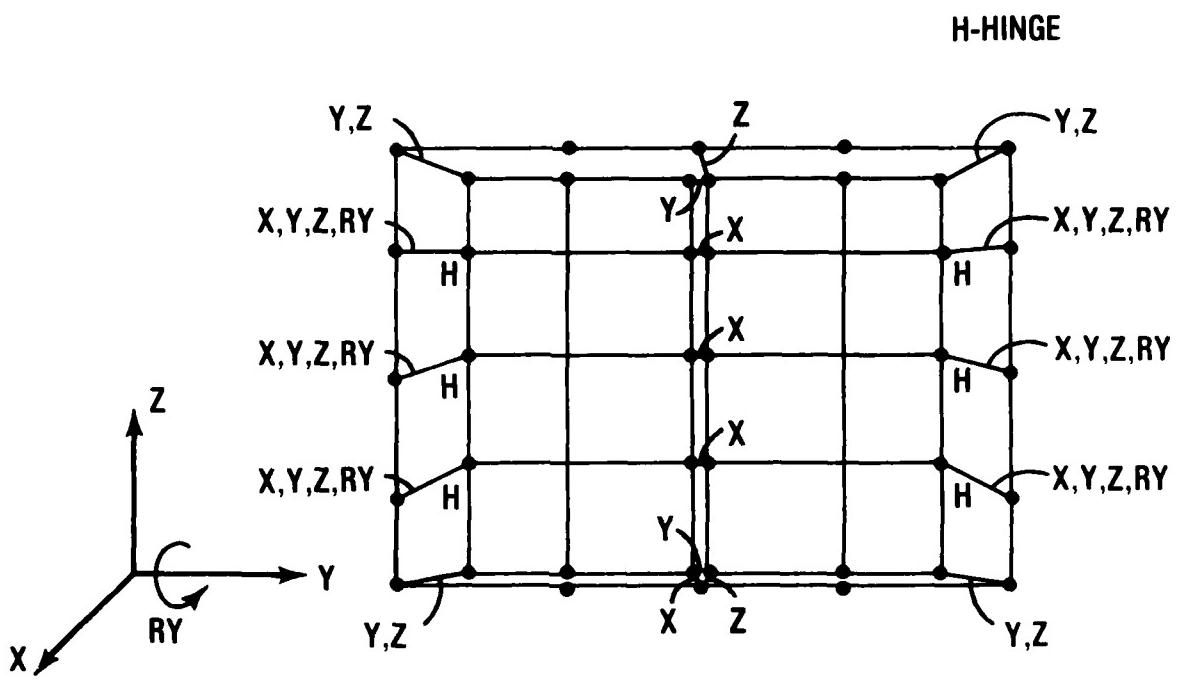
Figure 15. Case 5. Cargo door endwall, connected degrees of freedom between door and doorframe.
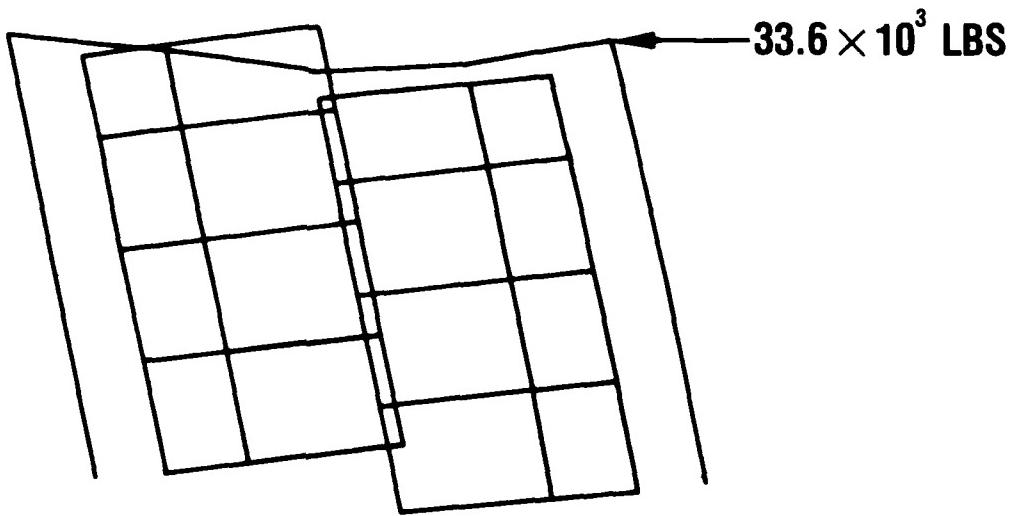
Figure 16. Case 5. Cargo door endwall, deformed body plot.
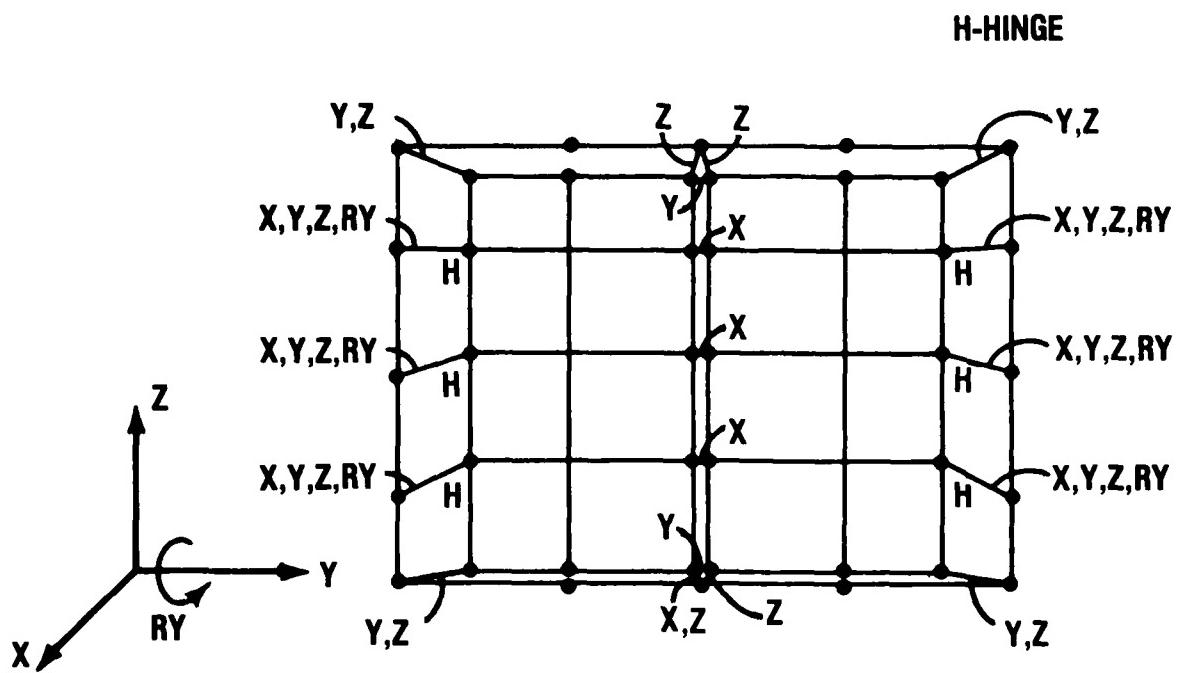
Figure 17. Case 6. Cargo door endwall, connected degrees of freedom between door and doorframe.
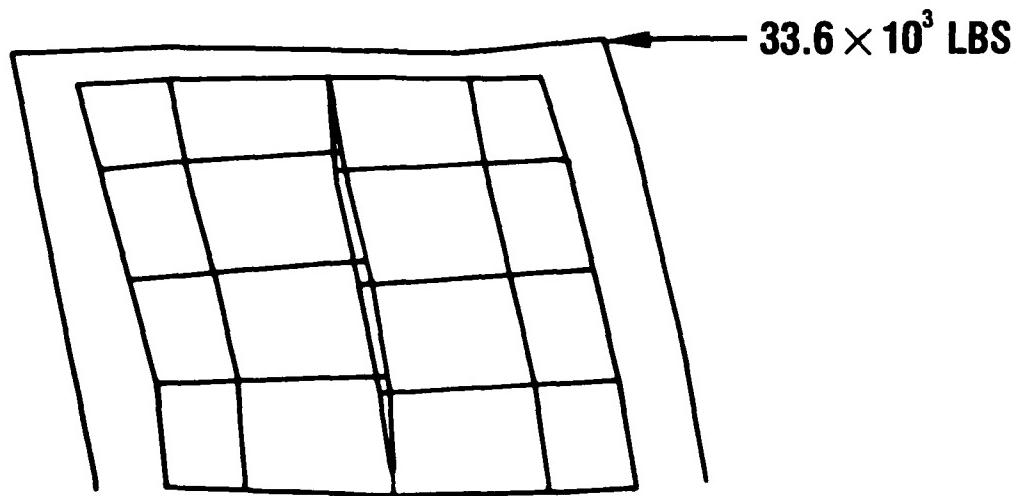
Figure 18. Case 6. Cargo door endwall, deformed body plot.
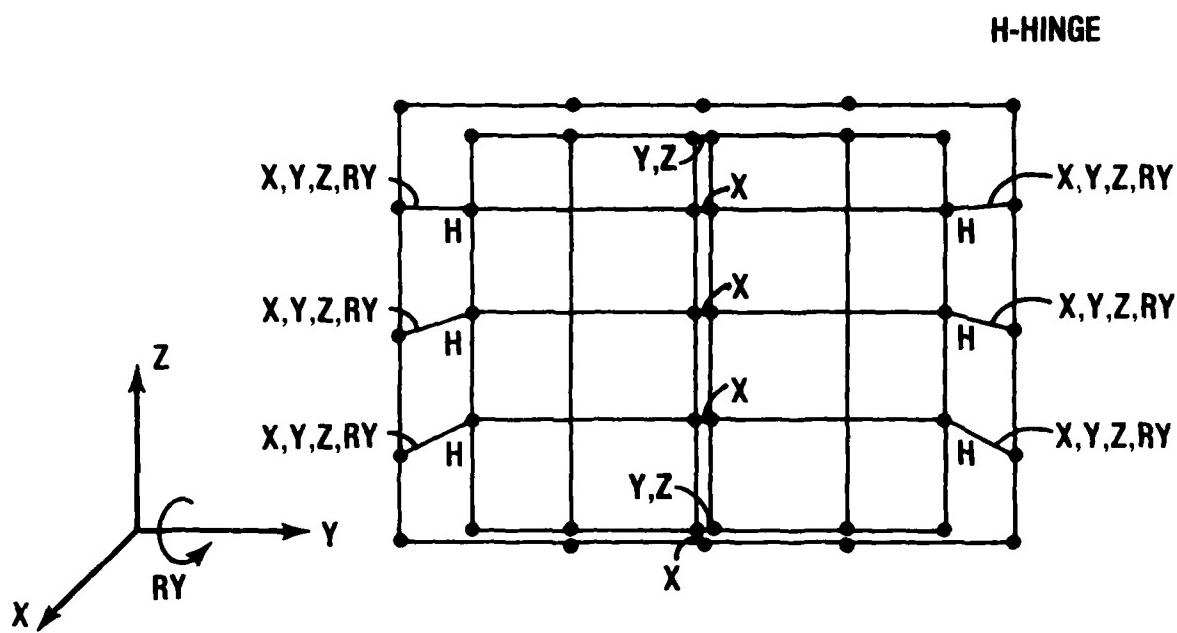
Figure 19. Case 7. Cargo door endwall, connected degrees of freedom between door and doorframe.
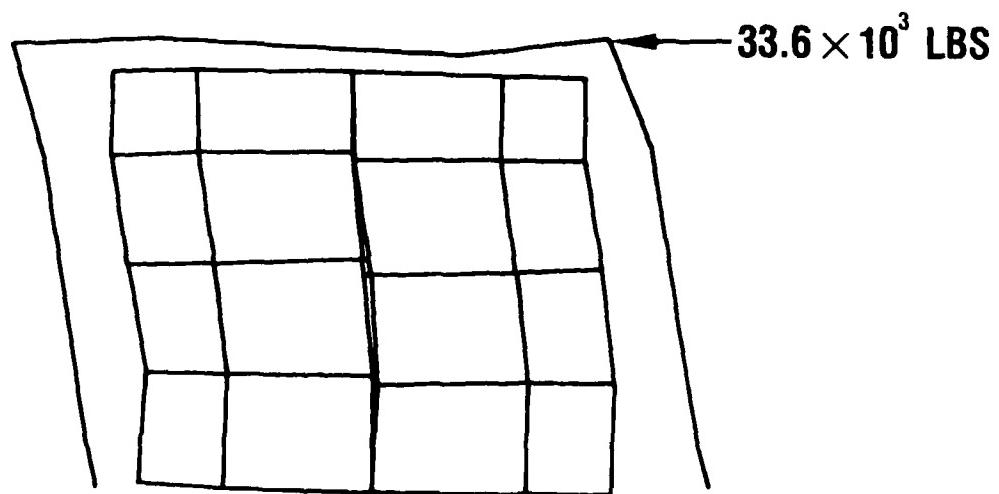
Figure 20.   Case 7. Cargo door endwall, deformed body plot.
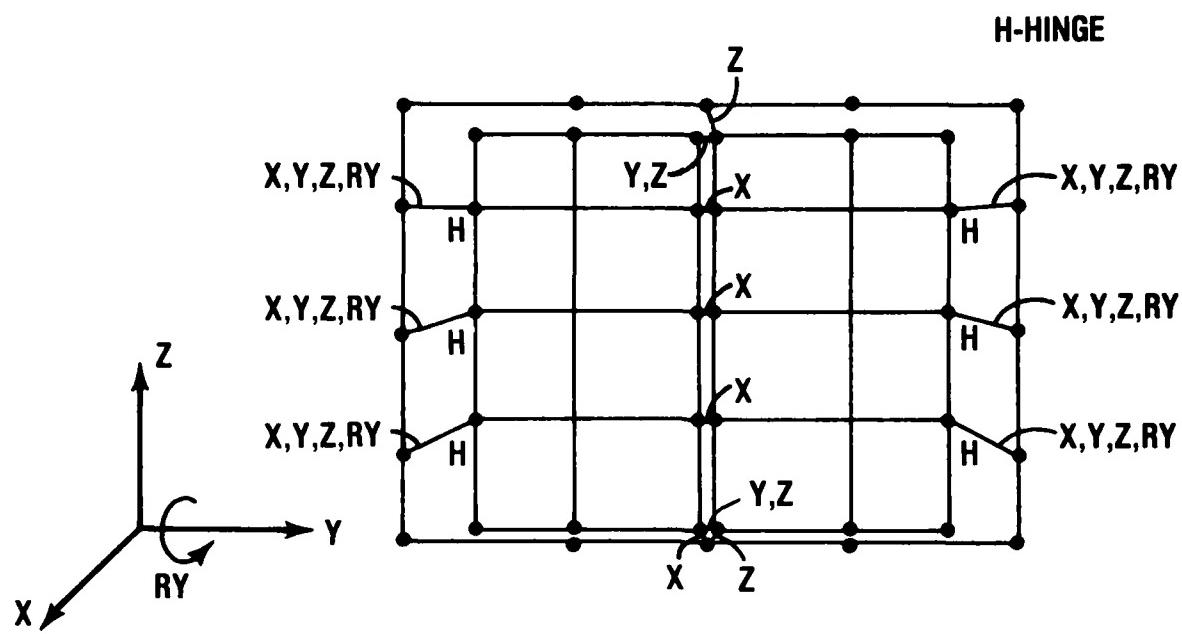
Figure 21.   Case 8. Cargo door endwall, connected degrees
of freedom between door and doorframe.
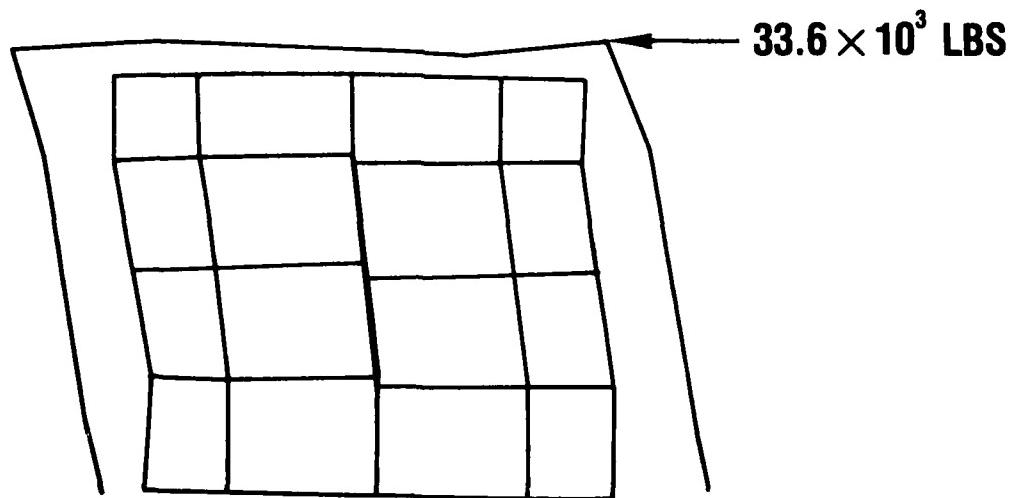
Figure 22.   Case 8. Cargo door endwall, deformed body plot.
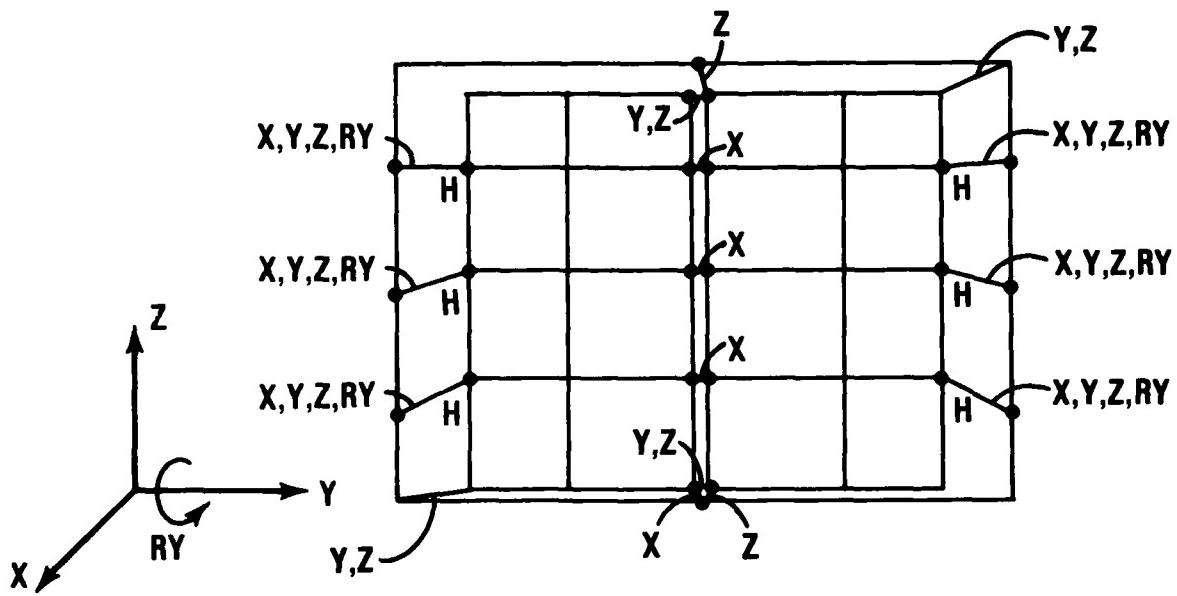
Figure 23.   Case 9. Cargo door endwall, connected degrees of freedom between door and doorframe.
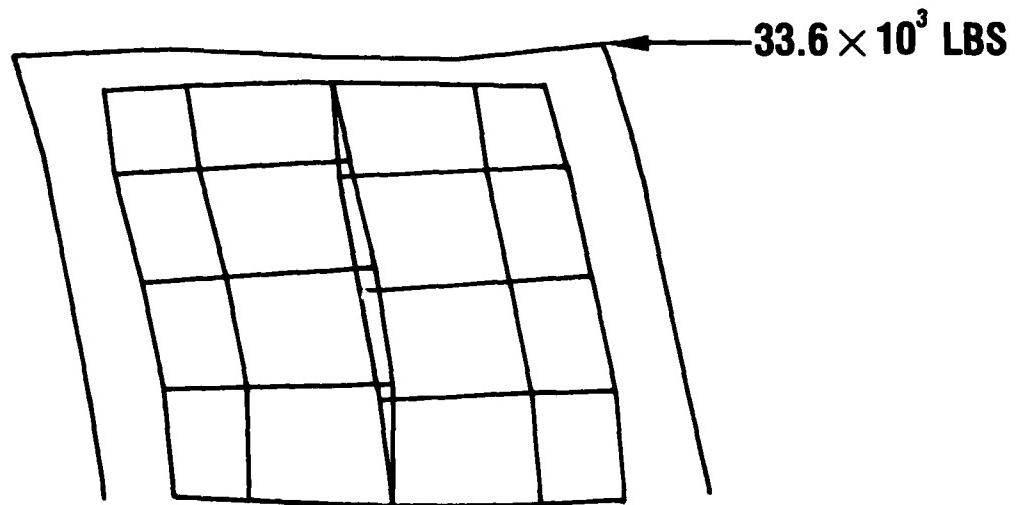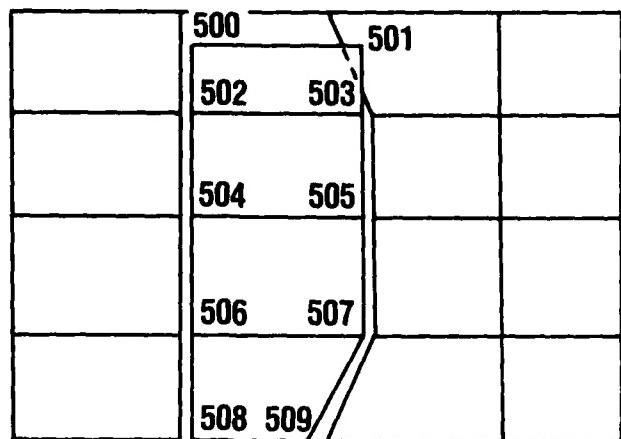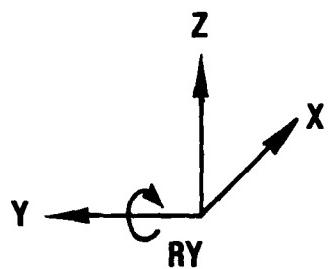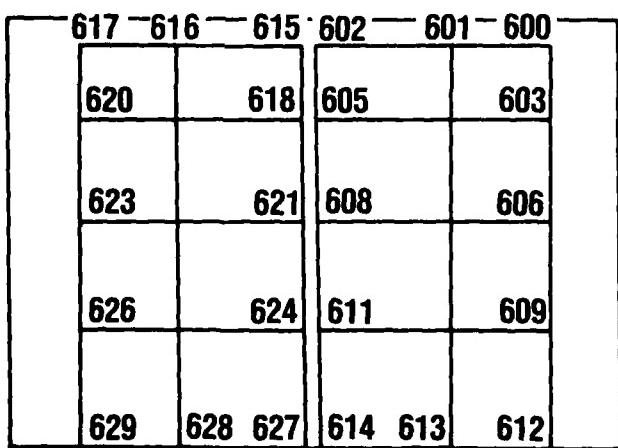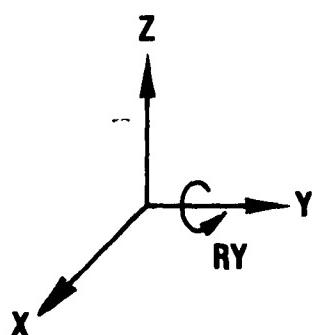
Figure 24.   Case 9. Cargo door endwall, deformed body plot.
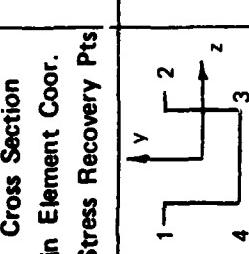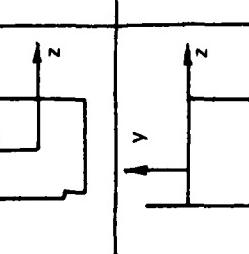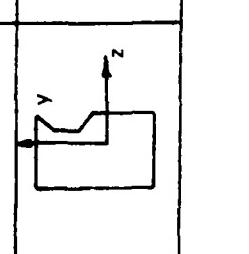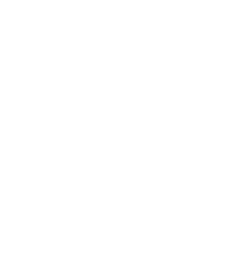
PERSONNEL DOOR END
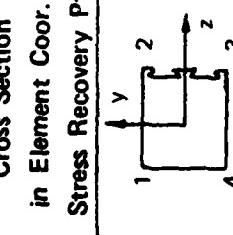
CARGO DOOR END

Figure 25.   Location of nodes on the boundry of the doors.

Table 2. Geometric properties for beam elements with property numbers 150, 170, 200, and 210

Property No.	Cross Section in Element Coor. Stress Recovery Pts	I_{zz} in⁴	I_{yy} in⁴	I_{yz} in⁴	A in²	J in⁴
150		5.39	1.75	0.0	1.72	0.01
170		0.26	0.27	−0.03	0.61	0.27
200		0.37	1.08	0.32	0.95	0.27
210		0.40	0.76	0.06	0.87	0.80

31

Table 3. Geometric properties for beam elements with property numbers
220, 300, 400, and 410

Property No.	Cross Section in Element Coor. Stress Recovery Pts	I_{zz} in^4	I_{yy} in^4	I_{yz} in^4	A in^2	J in^4
220		0.40	0.67	0.00	0.85	0.64
300		0.51	0.87	−0.18	0.99	0.64
400		1.03	0.62	−0.03	0.93	1.07
410		1.04	0.56	0.02	0.92	1.07

32

Table 4. Geometric properties for beam elements with property numbers
500, 510, 601, and 702
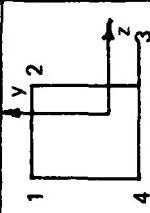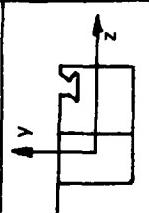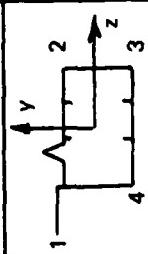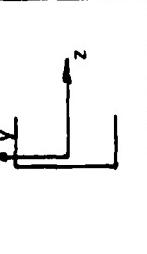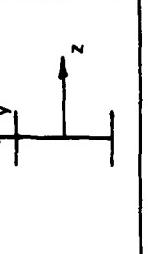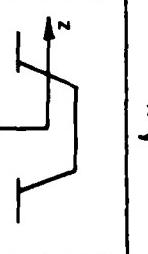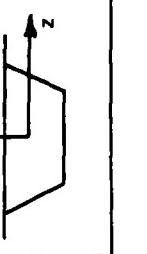
Property No.	Cross Section in Element Coor. Stress Recovery Pts	I_{zz} in⁴	I_{yy} in⁴	I_{yz} in⁴	A in²	J in⁴
500		0.63	0.67	0.27	0.90	0.46
510		0.49	0.34	0.03	0.77	0.63
601		1.34	6.07	1.06	1.74	2.36
702		29.01	40.21	0.43	7.76	51.99

33

Table 5. Geometric properties for beam elements with property numbers
703, 801, 802, 803, and 804

Property No.	Cross Section in Element Coor. Stress Recovery Pts	I_{zz} in^4	I_{yy} in^4	I_{yz} in^4	A in^2	J in^4
703		13.23	3.68	2.73	2.78	6.02
801		7.56	1.78	0.00	2.38	0.05
802		5.50	0.72	0.00	1.63	0.01
803		9.76	15.68	-0.01	3.06	0.02
804		28.0	187.	0.0	7.27	74.3

34

Table 6. Sample stress data for personnel door end, see Figure 5 for element locations

Element Number	Maximum Combined Bending and Axial Stress (10^3 psi) in Element	
	Case 1	Case 2
512	−69.1	−13.6
517	8.0	6.4
518	2.7	1.9
519	1.2	1.3
520	1.3	0.8
521	1.0	1.1
522	− 1.1	− 0.5
523	− 2.7	− 1.0
524	− 4.9	− 4.9
525	− 4.0	− 3.1
526	1.8	4.3
527	−14.6	4.3
528	−24.9	− 5.7
529	− 7.8	2.6
530	− 4.2	6.3
531	22.3	12.2
532	−30.3	− 3.4
533	− 4.7	− 1.8
534	5.7	− 1.7
535	12.3	7.2
536	−54.4	−21.0
537	57.3	− 6.3
538	−13.1	− 5.0

Table 7. Sample stress data for cargo door end, see Figure 4 for element locations

Maximum Combined Bending and Axial Stress (10³ psi) in Element

Element Number	*Case 3	*Case 4	Case 5	Case 6	Case 7	Case 8	Case 9
600	13.6	17.1	16.6	10.2	8.4	− 9.6	10.9
601	7.2	5.7	5.9	− 2.1	− 5.5	− 5.3	2.2
602	− 6.3	1.5	− 2.8	− 1.2	8.1	10.3	5.3
603	−15.2	1.1	−10.0	− 1.6	8.3	8.4	4.4
604	−55.3	−21.7	−63.4	−11.2	−24.4	−22.5	−15.7
605	−46.1	−38.2	−41.9	− 6.9	−13.9	−13.2	− 8.7
606	−34.9	−46.5	−27.7	− 8.2	−14.6	−15.8	− 7.2
607	62.9	63.0	−23.1	−10.1	−19.9	−21.7	− 9.3
608	13.7	13.7	− 3.8	− 3.3	−22.5	−22.5	− 3.9
609	− 5.6	2.2	− 2.3	1.8	−11.6	−11.5	0.8
610	−10.0	3.0	2.4	3.7	8.2	8.4	2.9
611	−19.8	3.3	− 2.1	5.6	7.5	7.4	5.9

*The properties of the header beam were I_{zz} = 4.59, I_{yy} = 10.2, I_{yz} = 0.0, A = 2.28, and J = 4.06 for these computer runs as compared to the values given in Table 4 which were used for the other computer runs.

Table 8. Forces on doorframe due to door hinges and door corners at personnel door end

Force (10^3 lb)

Node*	H—Hinge C—Corner	Case 1		Case 2	
		f_y	f_z	f_y	f_z
500	C	0.00	0.00	11.26	23.38
501	C	0.00	0.00	3.56	0.00
503	H	0.506	0.109	− 4.94	−10.86
505	H	−1.012	−4.673	− 2.47	− 6.80
507	H	0.506	4.564	− 3.65	− 6.52
508	C	0.00	0.00	− 3.74	0.00
509	C	0.00	0.00	0.00	0.81

f_y = component of force in global y direction

f_z = component of force in global z direction

*See Figure 25

37

Table 9. Forces on doorframe and between doors due to door hinges, door corners, and adjacent door at cargo door end

Forces (10^3 lb)

Node*	H–Hinge C–Corner	Case 1		Case 2		Case 3		Case 4		Case 5		Case 6		Case 7	
		f_y	f_z	f_y	f_z	f_y	f_z	f_y	f_z	f_y	f_z	f_y	f_z	f_y	f_z
Right door															
600	C	0.0	0.0	2.091	– 0.888	11.710	7.402	15.071	7.392	0.0	0.0	0.0	0.0	19.071	8.572
602	C	0.0	0.0	–1.278	0.0	– 0.454	–8.362	– 2.073	–14.475	0.031	–11.770	– 0.088	–11.540	– 6.879	–13.928
603	H	0.394	–0.369	8.093	6.414	– 0.212	3.841	0.521	4.317	18.404	11.528	18.552	11.493	1.536	3.667
606	H	–0.787	5.421	–0.563	3.916	– 0.773	4.995	– 1.122	5.858	– 2.542	– 0.482	– 2.459	– 0.491	– 0.545	4.366
609	H	0.394	–5.052	–1.610	4.059	– 1.180	4.850	– 3.935	7.442	–14.986	10.501	–14.922	10.684	– 6.978	9.254
612	C	0.0	0.0	–3.713	1.528	– 5.346	2.682	– 7.324	1.995	0.0	0.0	0.0	0.0	0.0	0.0
614	C	0.0	0.0	–3.019	–15.029	– 3.744	–15.408	– 1.139	–12.529	– 0.906	– 9.776	– 1.083	–10.145	– 6.206	–11.932
Left door															
615	C	0.0	0.0	1.278	9.306	0.454	0.0	2.073	14.577	– 0.031	11.770	0.088	12.010	6.879	13.607
617	C	0.0	0.0	5.920	– 3.356	– 1.234	0.511	11.021	– 6.407	0.0	0.0	0.0	0.0	0.0	0.0
620	H	–0.104	0.047	–0.139	– 0.904	3.279	– 0.561	0.944	– 2.183	19.820	– 3.720	19.688	– 3.656	9.569	– 3.516
623	H	0.207	0.073	–2.430	– 1.732	– 0.732	– 0.544	– 1.782	– 2.857	– 3.392	– 3.116	– 3.507	– 3.086	– 3.735	– 4.058
626	H	–0.104	–0.120	– 6.521	5.854	– 5.444	– 4.600	– 5.418	– 5.967	–17.304	–14.709	–17.352	–14.664	– 6.537	– 6.980
627	C	0.0	0.0	3.018	0.0	3.744	0.0	1.139	11.707	0.906	9.776	1.083	9.396	6.206	11.159
629	C	0.0	0.0	–1.127	2.542	– 0.067	5.195	– 7.976	– 8.870	0.0	0.0	0.0	0.0	–12.381	–10.212

*See Figure 25.

38